COMPENSATION OF WORKTABLE MOTION ERROR BY AN ACTIVELY CONTROLLED HYDROSTATIC GUIDEWAY

TOMAS LAZAK, EDUARD STACH, JAN SMOLIK, IVAN DIVIS, TOMAS FORNUSEK
Czech Technical University in Prague, Faculty of Mechanical Engineering, Department of Production Machines and Equipment (RCMT), Prague, Czech Republic
DOI: 10.17973/MMSJ.2022_12_2022155
t.lazak@rcmt.cvut.cz

The accuracy of machine tools is limited by many factors, such as geometric and thermal errors. Current error reduction approaches include e.g. volumetric compensation. However, if a machine tool has only linear axes, angular errors cannot be compensated since there is no controllable axis that could change the tool or workpiece inclination. Therefore, an actively controlled hydrostatic guideway was developed to compensate for angular and other geometric errors. This paper aims to experimentally verify the hybrid use of constant resistance and the pilot stage of an industrial proportional pressure relief valve for regulation of oil flow through hydrostatic pockets and control of these pockets as well as active compensation of machine tool geometric errors. The error reduction of the tested linear axis is presented.

KEYWORDS:
Hydrostatic guideway, machine tool, angular error compensation, straightness error compensation,

INTRODUCTION

One of the main manufacturer requirements is the accuracy of finished parts. Accuracy depends largely on the ability of machine tools to precisely position the cutting tool. Precise positioning is limited by geometric, thermal and cutting-force induced errors [Ramesh, 2000]. Geometric errors are caused by the inaccuracy of the machine parts and the assembly process. Thermo-mechanical machine tool deformation is the result of thermal loading by the normal spindle and axes' operation, heat from the cutting process, etc. [Bryan, 1990]. Expansion and distortion due to temperature changes lead to geometric errors. Positioning errors $\delta_x(x)$, $\delta_y(y)$ and $\delta_z(z)$ and straightness errors $\delta_y(x)$, $\delta_z(x)$, $\delta_x(y)$, $\delta_y(y)$, $\delta_z(y)$, $\delta_x(z)$, $\delta_y(z)$ and $\delta_z(z)$ can be compensated by the positioning of linear axes X, Y and Z. [Lee, 1998; Zhang, 2011]. However, in cases where a machine tool (MT) has only linear axes, the angular errors $\varepsilon_x(x)$, $\varepsilon_y(y)$ and $\varepsilon_z(z)$ and the squareness errors S_{xy}, S_{yz} and S_{xz} cannot generally be compensated [Schwenke, 2008]. Fig. 1 visualises the effect of angular error on a machined surface. Although the position of the tool centre point is compensated, the physical orientation of the tool remains unchanged because of the absence of an actuator that could alter the angle. This paper offers an approach to angular error compensation by means of actively controlled hydrostatic (HS) guideways.

Along with hydrodynamic and plain sliding guideways, hydrostatic guideways are essential sliding connectors for the moving parts of a machine tool. HS guideways utilize a thin layer of externally pressurized oil between moving surfaces. Generally, the design objective is to ensure constant thickness of the oil film (layer) between the guiding surfaces and HS pocket. On the contrary, the proposed system actively changes the thickness of the oil layer and thus tilts the machine parts in a controlled manner to compensate for angular errors. The thin layer of oil is referred to as a throttling gap height. The HS flow rate regulators can be divided into three gap height control groups. The first group contains passive components, e.g. flow dividers and hydraulic resistors such as capillaries and orifices. These regulators have limited control capabilities. Flow dividers have a high load carrying capacity and stiffness while the stiffness of hydraulic resistors is lower. Flow dividers are cost-intensive. In contrast, hydraulic resistors present a cost-effective solution [Slocum, 1992a; Weck, 1997].

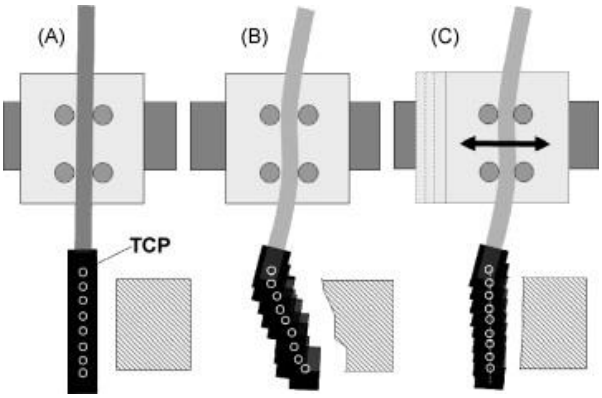

Figure 1. Effect of compensation for a three-axis milling machine: (A) zero geometry machine errors, (B) uncompensated geometry errors, (C) compensated position of tool centre point (TCP), uncompensated angular error [Schwenke, 2008]

Flow regulators from the second group use various mechanical feedback principles to maintain a constant throttling gap height. Progressive flow rate controllers are diaphragm valves with pressure feedback. When pressure in the HS pocket rises, flow through the controller increases. As a result, the throttling gap height tends to remain constant, and therefore the stiffness is superior to that of hydraulic resistors [Hyprostatik, 2022, 2021; Yang, 2014]. Self-regulating systems [Slocum, 1992b] make use of feedback by preliminary throttling and bypass to the facing HS pocket. Therefore, at least two hydrostatic pockets are required for gap height control. The final bearing stiffness is higher than with hydraulic resistors [Zollern, 2022; HUANG, 2013].

The last group contains systems with active throttling gap height control. These systems keep a constant throttling gap height, or the throttling gap height is freely controlled in the designed range. Servostatic guideways [Zeleny, 1969] use one mechanical position feedback for multiple HS pockets, which causes difficulties when the structure is deformed, e.g. by workpiece weight, because the system attempts to act upon the incorrect position feedback of individual pockets. Nevertheless, stiffness is increased significantly [Zeleny, 1973]. Actively controlled capillaries [Park, 2006] are piezoelectric valves with controllable hydraulic resistance. Feedback is electrical. Actively controlled capillaries are suitable for precise applications [Park & Lee, 1998]. Another approach is to control flow through the HS pocket by changing oil viscosity. In this approach, magnetorheological fluid is suitable since its viscosity depends on the intensity of magnetic flux. Thus, flow rate is controlled by magnetic field in the HS pocket and its proximity. The benefit is the very fast reaction [Hesselbach, 2003; Guldbakke, 2006; Abel-Keilhack, 2004; Patzwald, 2001]. Finally, systems with an electronic

closed loop can control the flow rate through HS pockets by utilizing hydraulic valves [Nakao, 2015] or servovalves [Renn, 2019].

HS guideway control was experimentally verified in [Lazak, 2016]. The gap height was controlled by hydraulic resistance connected in parallel with a proportional pressure relief valve. The cited paper shows the tilting of the worktable and its positioning in a direction perpendicular to the guiding prisms. However, the worktable remained in one position of the axis stroke due to construction limitations.

This paper presents further investigation of actively controlled HS guideways applied as a geometrical error compensation device. A new linear axis was designed and built. Then geometrical errors were measured and compensated. The error reduction is presented and the results are discussed with respect to the accuracy of state-of-the-art machine tools. Published accuracy errors of mid-sized machined tools were used for this purpose. Straightness errors of linear axes range up to around 10 µm. Angular errors of linear axes range up to higher tens of $\mu m/m$ [Holub, 2015, 2020; Kenno, 2020; Liang, 2020; Wei, 2019].

2 ACTIVE HYDROSTATIC GUIDEWAYS

The objective of developing actively controlled HS guideways was to achieve a micro meter and micro radian range controlled movement of e.g. the worktable of a mid-sized vertical milling centre without adding any compliant (flexible) parts into the machine – tool – workpiece kinematic chain. These microscopic movements are intended to serve as a correction of geometric errors and thermal deformations which manifest as angular errors that cannot be compensated on three-axis machine tools and therefore impair the working accuracy of the machine. The worktable movement is achieved by active control of individual hydrostatic pockets' throttling gap heights in each corner in the vertical direction. Although a hydrostatic linear axis can generally have any number of HS pockets in the vertical direction, in this chapter where we describe the working principle, we will assume only four pockets, one in each corner of the working table. The active hydrostatic guideway consists of three main sections: the hydrostatic guideway, hydraulic system and control system.

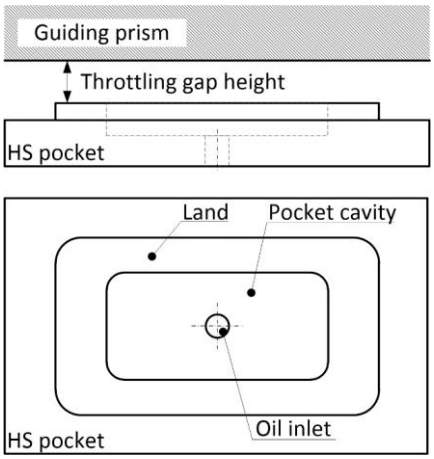

Figure 2. Hydrostatic pocket

2.1 Hydrostatic guideways

A hydrostatic guideway consists of HS pockets and guiding prisms. Fig. 2 shows one HS pocket. Pressurized oil flows from the regulator through an oil inlet to a pocket cavity. The oil fills the cavity and flows out over the land through a narrow gap. The throttling gap is a hydraulic resistance which provides a bearing pressure in the pocket cavity. The throttling gap height, certainly a distinctive dimension (usually tens of µm), is dependent on the HS pocket dimensions, oil viscosity, load, and flow through the HS pocket.

The HS pocket dimensions can be changed only during the design phase and thus can be considered constant. Load and oil viscosity are disturbance variables. Therefore, gap height is a non-constant function of flow through the HS pocket.

Generally, the flow rate regulators for HS guideways are designed to keep the throttling gap height constant. This goal is met with varying success depending on the regulator type [Stach, 2013]. With an actively controlled HS guideway, the goal is to control the gap height.

2.2 Hydraulic system

Fig. 3 shows the hydraulic circuit that enables control of the throttling gap height. A proportional pressure relief valve PV is connected in parallel to capillary C_1. When the valve is fully closed, the oil flows only through the capillary and the throttling gap height is given by the capillary resistance. This default state ensures that the HS guideway will always work and moving surfaces will not come into contact and damage each other. By the proportional opening of the valve PV, the oil flow to the HS pocket is increased and the gap height (h_a) rises.

The parallel connection of the capillary is crucial because it has a stabilizing effect on flow rate. A more suitable option than the pressure relief valve would be a 2-way proportional flow control valve, which has superior precise flow control and has the advantage of knowledge of the pressure-flow characteristic. The disadvantage of the flow control valve is its higher price.

For each controlled HS pocket, one valve is needed. Therefore, at least four valves are required for a linear machine tool axis if we assume pockets only in the corners of e.g. a worktable. These actively controlled HS pockets may be used for positioning the worktable perpendicularly to the guiding surfaces (prisms).

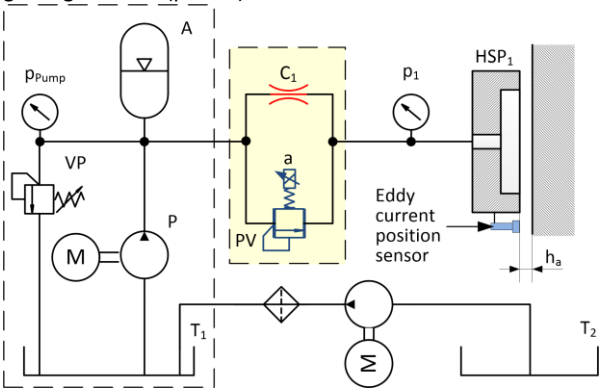

Figure 3: Hydraulic circuit for gap height control with capillary bypassing proportional valve

It is apparent that controlling multiple hydrostatic pockets with flow control valves may be significantly more expensive than application of a pressure relief valve. A new linear axis was designed to test actively controlled HS guideways for the purpose of geometrical error compensation. A suitable pressure relief valve was SR1P2-A2. On the contrary, a suitable flow control valve would be DUR1,6L06PK11.

The test linear axis consists of a bed with guiding surfaces (prisms) and a worktable that is equipped with four HS blocks. Fig. 4 illustrates the HS guideway scheme and hydraulic connection. A HS block (also known as a Hydrostatic guide shoe by HYPROSTATIK Schönfeld GmbH when equipped with PM flow regulators) is a precision machined part containing three HS pockets. The first HS pocket (the main HS pocket) provides the load-carrying capacity for the table. With a real

machine tool (MT), this pocket would mainly carry the weight of the workpiece. The second (lateral) HS pocket bears forces acting in the horizontal direction, for example inertial forces during acceleration of the perpendicular axis of a real MT. The third HS pocket provides preloading of the main HS pocket in order to increase the stiffness of the guideway.

With the state-of-the-art MT hydrostatic linear axis, the gap heights (flow rate through the HS pocket) would be regulated, for example, by a combination of PM regulators and capillary as depicted in Fig. 4 (green box). In this case, the gap height characteristics are given by the design parameters of the PM regulator Q_0 and K_r. The gap height cannot be controlled; its characteristics have been predetermined to be a nonlinear function of the load.

In the case of active regulation, the PM regulator of the main HS pocket is replaced by a proportional valve and capillary as shown in Fig. 4 (blue box). Capillary C_1 ensures minimum gap height. The proportional opening of the valve PV causes an increase in oil flow rate and therefore an increase in gap height. In order to provide vertical clearance (play) of the table for the compensation to work, the HS guideway must work with higher throttling gap heights to provide sufficient space for the HS block to move. The greater throttling gap height results in higher oil flow (which can be counteracted by higher oil viscosity), and lower stiffness than what could be achieved with PM regulators.

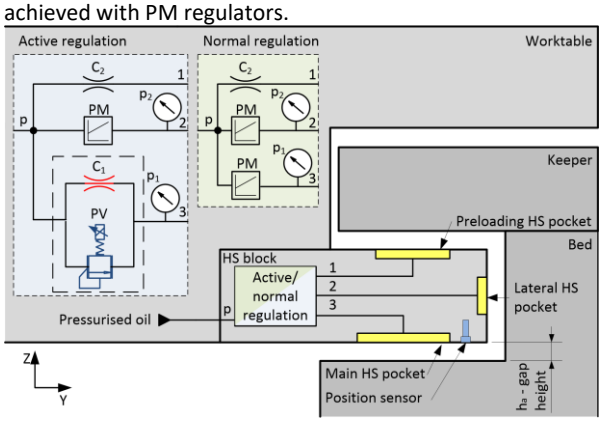

Figure 4. Closed HS guideway of test linear axis

2.3 Control system

Fig. 5 shows the feedback control schematics of an active HS guideway supplemented by a coordinate system in Fig. 6. The initial gap height h, which would be measured in the middle of the table, is set to the middle of the vertical height regulation range. Thus, the maximum tilt can be reached.

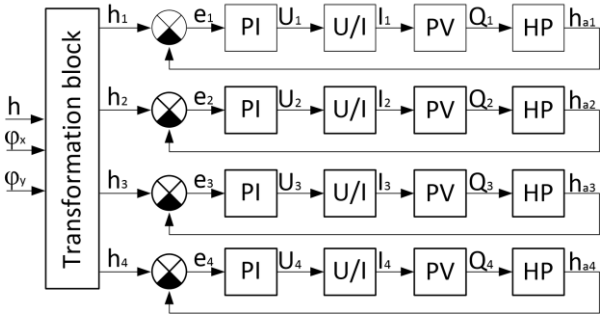

Figure 5. Control schematic for four HS pockets

When compensations are enabled, φ_x and φ_y, the corrective tilts of the worktable about the X and Y axes are tabular functions of worktable position X. The gap height setpoints at the corner HS blocks (h_1 to h_4) are calculated by the transformation block to satisfy the required φ_x and φ_y. The actual gap height (h_{a1}) is measured with an eddy current sensor (Fig. 4). A regulation error e_1 is calculated by $e_1 = h_1 - h_{a1}$. The regulation error is an input for the PI regulator of each active pocket. A voltage output of PI regulator is fed to a PWM amplifier (U/I) that powers the proportional valve (PV) coil. As a result, flow rate through the proportional valve is changed and eventually the gap heights of the hydrostatic pockets (HP) h_{a1} to h_{a4} are reached.

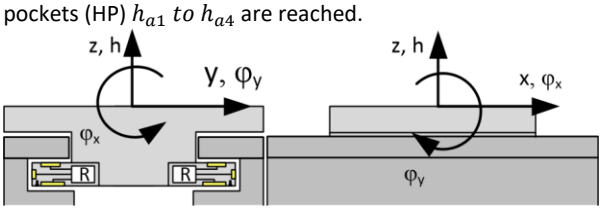

Figure 6. Coordinate system of the test linear axis

One of the key components of the regulation system is the gap height sensor. The gap height sensor is the position sensor that measures the relative distance between the HS block and guiding surface (prism), as can be seen in Fig. 4. Since the working environment is filled with hydraulic oil at alternating temperatures, only an eddy current sensor is able to operate at an acceptable precision of approximately 0.01 mm in the temperature range 10 – 30°C.

3. MEASURING SETUP

This chapter describes the measuring setup used for verification of the control range of the throttling gap height and therefore the worktable tilt range. Furthermore, the chapter describes the setup for measurement of geometrical errors of the tested linear axis.

3.1 Test bench

The test bench is based on the x-axis of a mid-sized vertical machining centre and therefore, results obtained from the experiment are directly applicable to machine tools. The dimensions that are critical for actively controlled HS guideways will be listed in this paragraph. The position of the HS blocks and maximum gap height affect the worktable tilt range. For a constant maximum gap height, the higher the distance between the HS blocks, the lower the tilt range.

The test bench consists of a worktable with HS blocks and a bed with guiding surfaces (Fig. 7). The worktable width and length are $700\ mm$ and $600\ mm$ respectively. There are four HS blocks in all, one in each corner of the worktable. The HS block width, length and height are $100\ mm$, $130\ mm$ and $50\ mm$ respectively. The distance between the HS blocks and position of the sensors is clear from Fig. 8. The stroke of the original machine tool axis was decreased to $600\ mm$ for cost reduction. The other critical dimensions remained unchanged.

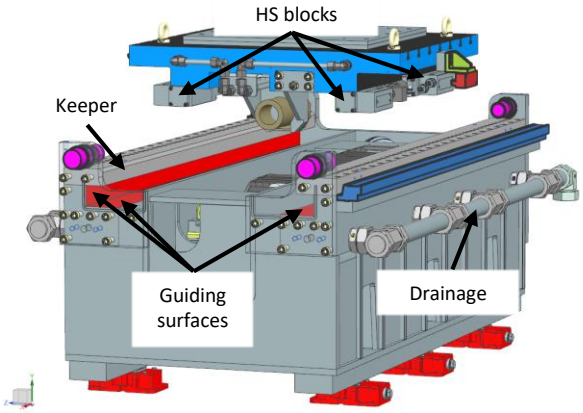

Figure 7. CAD model of the test bench

The HS guideway of the test bench is a closed type since it contains keepers for preloading. The keeper limits the maximum vertical displacement of the worktable (see Fig. 4 and Fig. 7.). Assuming that the worktable lies on the guiding surfaces h_a = 0, clearance between the HS block (its

preloading pocket) and the keeper limits the maximum displacement of the worktable. The designed clearance of the tested HS guideway was 100 µm. The initial oil film thickness was designed for h_a = 45 µm. The initial oil film thickness is given by the resistance of capillaries C_1 and C_2 (Fig. 4), HS block dimensions and the clearance.

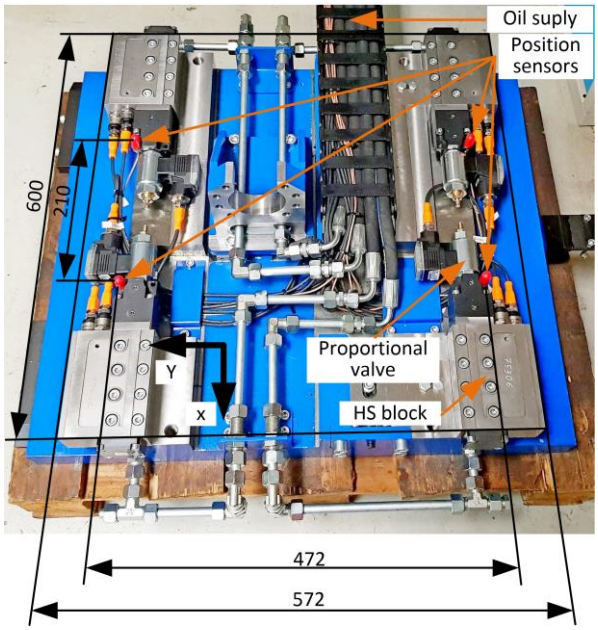

Figure 8. Bottom view of worktable

The test bench dimensions and geometrical errors were measured by a coordinate measuring machine and are summarized in Fig. 9. The height of the HS blocks was $50\ mm$ with a deviation of less than $2\ \mu m$. The clearance of the guideway was higher than the theoretical value of $100\ \mu m$. The clearance was approximately $114\ \mu m$ and $109\ \mu m$ which was an acceptable deviation. The flatness error of both guiding surfaces for the main HS pockets was $6\ \mu m$. There is also a parallelism error between the keeper and the bed which causes a change in clearance as the X coordinate changes. Furthermore, the straightness of guiding surfaces for the main HS pockets was measured after the bed was adjusted on the foundations. XM-60 was used for this measurement. The measured straightness was $1.5\ \mu m$ and $2\ \mu m$ and it had a U-shape. The flatness error of the surface where the HS blocks are connected to the worktable was $5\ \mu m$. The listed errors are within the tolerance but the errors contribute to the overall error of the linear axis.

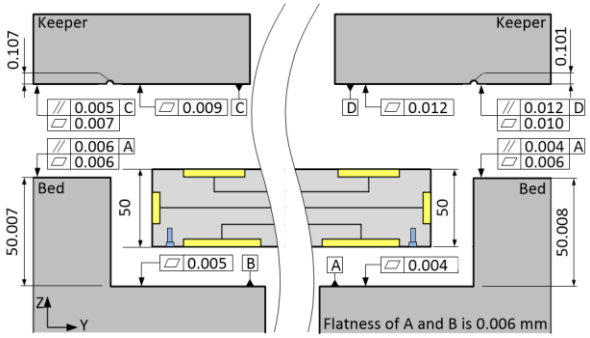

Figure 9: Measured test bench dimensions and geometric errors

The hydraulic supply provides hydraulic oil to the HS blocks through four independent hoses and pipes (Fig. 8). The supply pressure was $50 \pm 1\ bar$ and the oil temperature was $24 \pm 0.4\ °C$. The oil viscosity class was ISO VG 68.

3.2 Measurement of vertical displacement

When the HS guideway is not pressurized, the worktable lies on the guiding surface of the prisms. Then, when oil pressure rises, the worktable moves upward in the direction perpendicular to the axis stroke. This vertical displacement h was measured by an external contact position sensor in the middle of the worktable, as shown in Fig. 10. A contact position sensor T102F from PETER HIRT GmbH was used. The sensor linearity error is 0.25% in the range $\pm 1mm$ at a temperature of $20\ °C$ and repeatability is $0.01\ \mu m$. The vertical displacement was measured in the middle of the worktable.

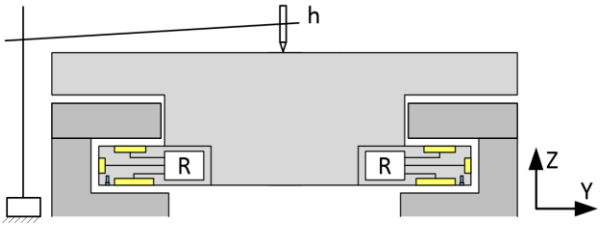

Figure 10. Schematic of measurement of worktable vertical displacement

Besides the vertical displacement h, displacements $h_{a1}\ to\ h_{a4}$ measured by internal sensors in each HS block in the worktable corners were measured by the active hydrostatic guideway control system. A sensor EPRO PR6422/000, accompanied by a signal converter CON041, was used. Their range is $1\ mm$ and the maximum linearity error is below $\pm 1.5\%$. The temperature error is less than $2\%/100\ K$.

3.3 Measurement of worktable tilt

The worktable tilt was measured by an electronic level Minilevel NT/11 from Wyler AG. For the measured range, $\pm 150\ \mu m/m$ is the maximum error of the measurement $\pm 1.5\ \mu m/m$. The tilt about the X and Y axes, denoted as $\varphi_x\ and\ \varphi_y$, was measured as depicted in Fig. 11.

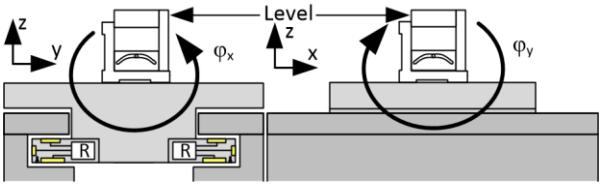

Figure 11. Tilt measurement by electronic level

3.4 Measurement of geometrical errors

Geometrical errors were measured by a Renishaw XM-60 laser measurement system (Fig. 13). The XM-60 enables simultaneous measurement of errors in six degrees of freedom along the linear axis. In our case, straightness errors $\delta_y(x)$, $\delta_z(x)$ and angular errors $\varepsilon_x(x)$, $\varepsilon_y(x)$, $\varepsilon_z(x)$ were measured. The errors are depicted in Fig. 12.

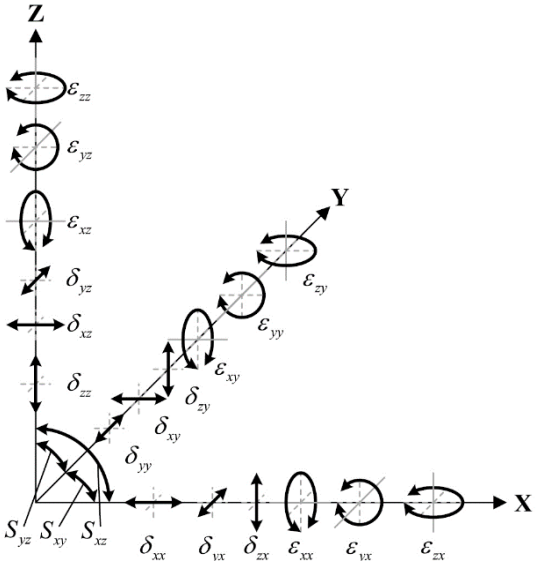

Figure 12. Twenty-one geometric errors of a three-axis machine (Li, 2020)

Since changes in air pressure, temperature and relative humidity can affect measurement accuracy, the XC-80 compensator was used for compensation of environmental changes. Accuracy XM-60 parameters are summarized in Table 1.

	Position	Angle (yaw/pitch)	Straight-ness	Angle (roll)
Accuracy	±0.5ppm	$\pm 0{,}001A$ $\pm$ (0,5 $+ 0.11M)\mu rad$	$\pm 0{,}01B$ $\pm 1\mu m$	$\pm 0{,}01A$ ±6,3 μrad
Resolution	1nm	0,03 μrad	0,25 μm	0,12 μrad
Range	0 to 4 m	±500 μrad	±250 μm radius	±500μrad
A-indicated value, M-measured distance in m, B-indicated straightness value				

Table 1. Laser measurement system (XM-60) accuracy parameters

The tested linear axis is depicted in Fig. 13 and Fig. 14. The laser launch unit was connected to the bed and the receiver was moving with the worktable.

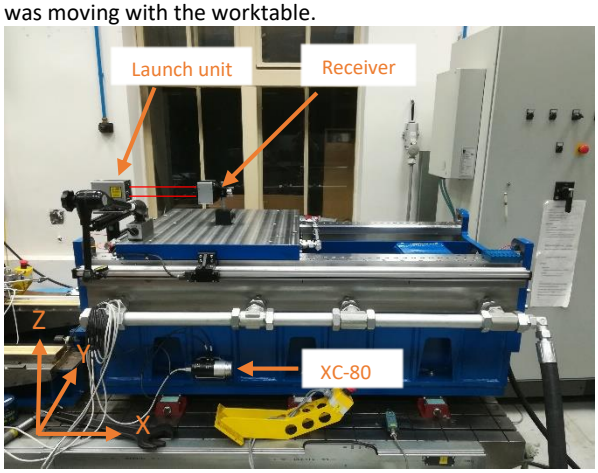

Figure 13. Linear axis error measurement by XM-60, position of axis X = 0

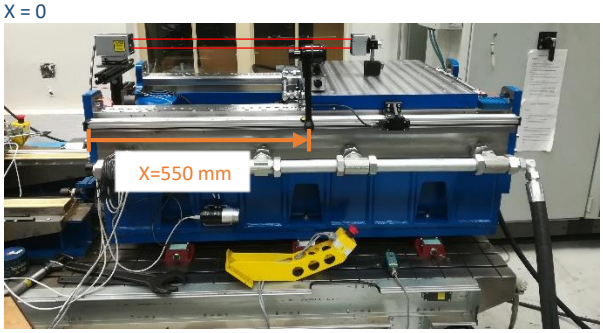

Figure 14. Linear axis error measurement by XM-60, position of axis X = 550

3 COMPENSATION SYSTEM PERFORMANCE

3.1 Accuracy of vertical positioning

When the HS guideway is not pressurized, the worktable table lies on the guiding surface of the prisms. Then, when oil pressure rises, the worktable moves upward in the direction perpendicular to the axis stroke. This vertical displacement was measured.

3.1.1 Vertical positioning at constant X position

The worktable was moved to position $X = 250\,mm$ (approximately to the middle of the X axis). The vertical displacement rose from $60\ \mu m$ to $120\ \mu m$ and then dropped back down. The vertical displacement was set by increments of $5\ \mu m$. The set gap height of $120\ \mu m$ is higher than the measured clearance of $109\ \mu m$. The higher gap height is possible due to the elastic deformation of the keeper and the bed. The regulation system had enough time to reach the set position so the measurement was quasi-static. The set and measured vertical displacements are shown in Fig. 15.

The maximal difference between the set and the measured absolute displacement was $2.3\ \mu m$. A small hysteresis of approximately $1\ \mu m$ is apparent from the measured data. The positioning range in the vertical direction is $60\ \mu m$, which means the throttling gap height ranges from $60\ to\ 120\ \mu m$. Assuming the vertical displacement is an MT axis, the mean bi-directional positioning deviation in the whole range of vertical movement evaluated according to ISO 230-2 yields $\bar{B} = 2.7\ \mu m$.

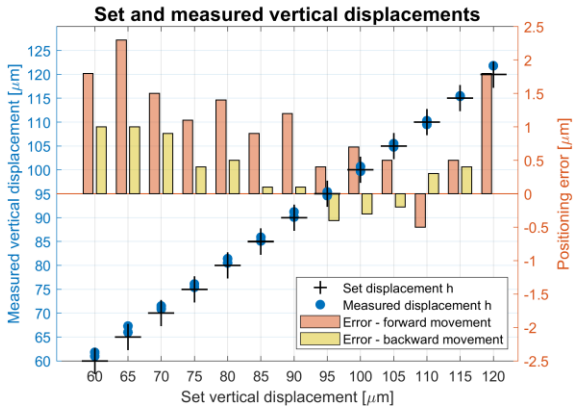

Figure 15. Set and measured vertical displacements

3.1.1 Straightness error for various vertical displacements over the axis stroke

The vertical displacement of the worktable was set to $60\ \mu m$. Then $\delta_z(x)$ (vertical straightness error of the worktable movement along the axis stroke) was measured using the Renishaw XM-60 device. The worktable moved in $50\ mm$ increments. The same measurement was performed for several different vertical displacements (60; 80; 100; 110; 120 μm). For comparison, the measurement was performed also for passive regulation by capillary C_1 (see capillary in Fig. 4) when the proportional valves were fully closed. The measurement results are displayed in Fig. 16.

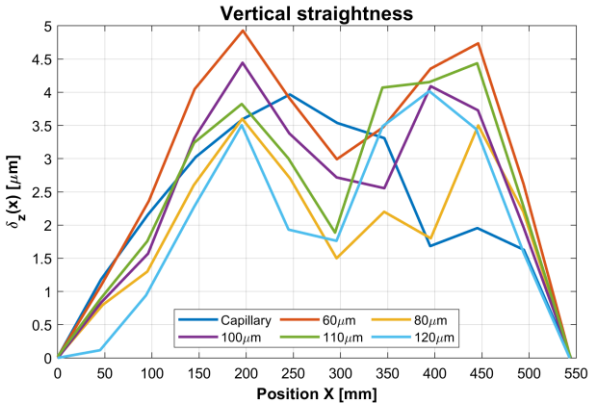

Figure 16. Vertical straightness of tested linear axis for various vertical displacements

The measured maximum vertical straightness error $\delta_z(x)$ of the tested linear axis was $5\ \mu m$. The difference in straightness for various vertical displacements was small. The difference is close to the measurement error of the XM-60. The vertical straightness error of the actively controlled HS guideway is comparable to the vertical straightness of the regular HS guideway regulated by the capillary. The straightness was measured without any compensation that could improve the straightness.

Fig. 17 shows the gap heights measured by the regulation system. The plotted data are again quasi-static. The set gap heights were reached for all gap heights except for $120\ \mu m$. In the case of $120\ \mu m$, the pump is not able to provide enough oil flow at the required pressure level, which marks

the end of the regulation range. However, overall straightness does not deteriorate. Nevertheless, the vertical straightness was measured without any load. It can be assumed that if a full load is applied, the gap heights would not be reached in the case of 120 μm vertical displacement. The gap heights are also plotted for regulation by capillaries (fully closed PV valves).

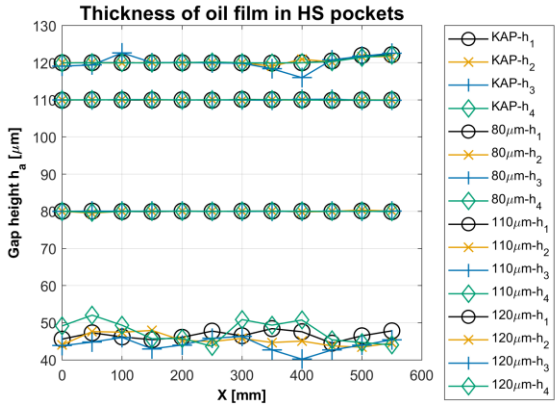

Figure 17. Measured gap height

Fig. 18. shows pressure measured in the main HS pockets. The pressure changes with the X coordinate.

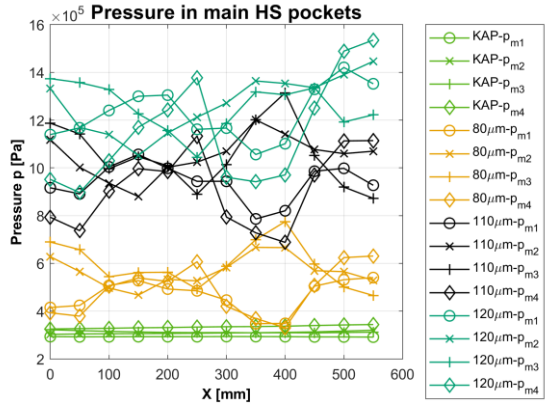

Figure 18. Pressures measured in main HS pockets

4.2 Tilt accuracy

The tilt accuracy was measured in the middle of the axis stroke and over the whole axis stroke.

4.2.1 Tilt accuracy in the middle of axis stroke

The worktable was moved to position $X = 300\,mm$ and vertical displacement was set to 85 μm. Then the worktable was tilted about the X axis from $\phi_x = 0$ to $\phi_x = 150\ \mu m/m$ and then to $\phi_x = -150\ \mu m/m$ and finally back to $\phi_x = 0$ in increments of 10 $\mu m/m$. We may assume the angle ϕ_x as a correction of angular error $\varepsilon_x(x)$ and respectively ϕ_y as a correction of $\varepsilon_y(x)$. The tilt was measured by the electronic level. The comparison of the set and measured tilt is shown in Fig. 19. The maximum difference between the set and measured values is 2 $\mu m/m$.

Analogously, a test was performed with the table tilting about the Y axis. The range was from $\phi_y = -150\ \mu m/m$ to $\phi_y = 150\ \mu m/m$. The maximum difference between the set and measured values is 4 $\mu m/m$. There is a higher hysteresis in the second case.

The tilt error is partially caused by the accuracy of position sensors that measure the oil layer thickness. The distance between the position sensors in the X direction is less than half of the distance between the position sensors in the Y direction (see Fig. 8). Therefore, the error in the measured gap height effects the tilt about the Y axis more than the tilt about the X axis. The tilt error about the Y axis is approximately double the tilt error about the X axis.

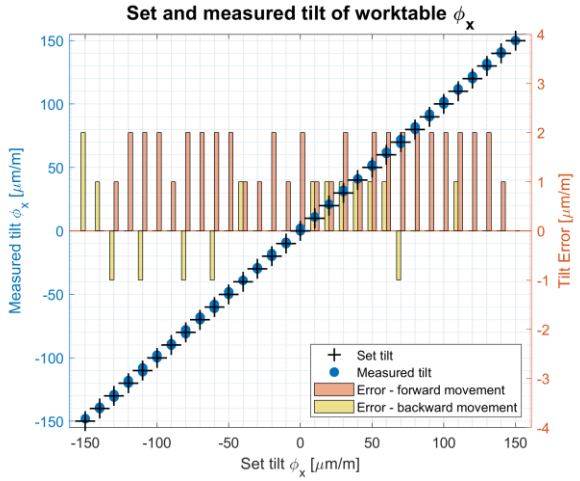

Figure 19. Comparison of set and measured worktable tilt

The tilt range $\pm 150\ \mu m/m$ is the same in both cases. The measurements were performed without any load.

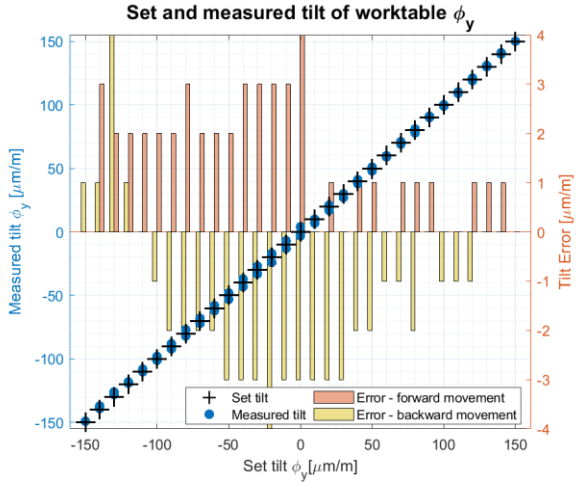

Figure 20. Comparison of set and measured worktable tilt

4.2.2 Tilt range over axis stroke

In this experiment, the worktable was moving from $X = 0\,mm$ to $X = 550\,mm$ in 50 mm increments while holding a set tilt angle of ϕ_x *or* ϕ_y. Each of the actively controlled hydrostatic pockets was kept at a constant set value during the measurements, resulting in a specified worktable tilt angle. In this experiment, these tilt angles ϕ_x *and* ϕ_y are perceived as a corrective movement of the compensation system. Therefore, the tilt angles are not denoted as errors although angular errors of the X axis were in fact measured with the Renishaw XM-60. The results of the ϕ_x measurement are presented in Fig. 21. The measured data for $\phi_x = 50\ \mu m/m$ were corrupted.

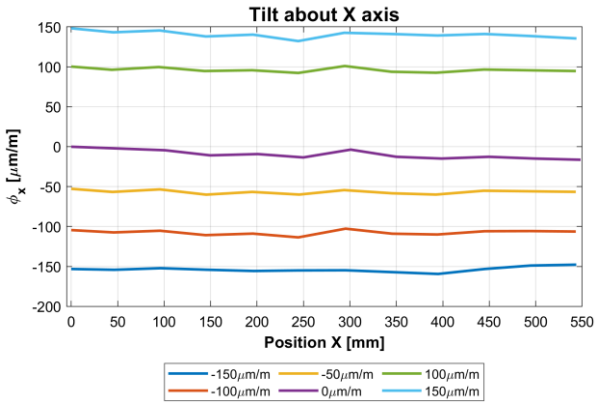

Figure 21. Tilt about X axis

The results of the ϕ_y measurement are presented in Fig. 22. The results above show that the active hydrostatics system is capable of reaching ϕ_x *and* ϕ_y in the range of $\pm 150\ \mu m/m$. This range is, however, specific to the tested structure as it is dependent on the distance between the HS pockets and their vertical range. The average error of ϕ_x *and* ϕ_y across the whole axis length is $-6.8\ \mu m/m$ and $16\ \mu m/m$ respectively. The error also includes errors of the mechanical structure, which exhibits geometrical and dimensional errors due to manufacturing accuracy and thermal deformations. Especially in the case of ϕ_y, there is a pattern that repeats for each tilt as can be observed from the results in the range from $X = 250$ to $X = 550\ mm$. The measurement was quasi-static without any load. Thus, the tilt error is not caused by quick changes. The vertical straightness error was almost the same for all measured tilts of the worktable.

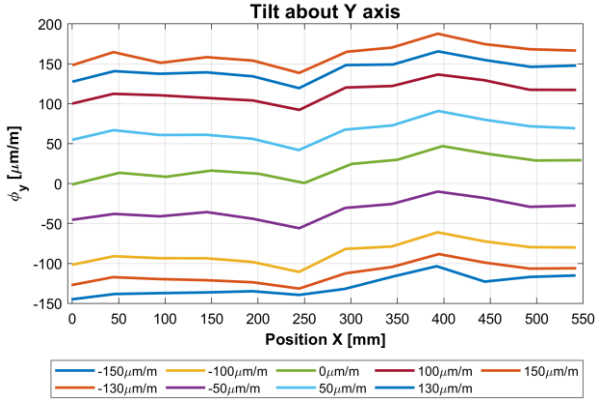

Figure 22. Tilt about Y axis

5. COMPENSATED AXIS

The following chapter describes the compensation tests of the X axis geometrical errors $\varepsilon_x(x)$, $\varepsilon_y(x)$ and $\delta_z(x)$.

5.1 Angular error compensation

In order to test the ability of the active hydrostatic guideway to compensate angular errors, information about the error magnitude first has to be established. A measurement of an error could be used as feedback but in our case a look-up table with corrective tilts ϕ_x *and* ϕ_y has been prepared as an inverse value of the measured angular errors $\varepsilon_x(x)$, $\varepsilon_y(x)$.

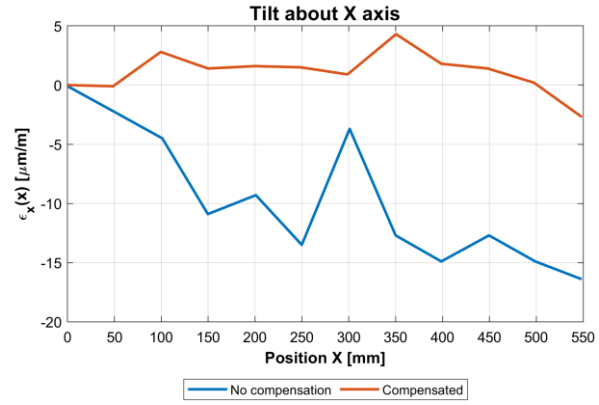

Figure 23. Comparison of tilt error for uncompensated and compensated axis

The errors were measured with 50 mm increments across the whole axis. The vertical straightness error $\delta_z(x)$ was not compensated. A comparison of compensated and uncompensated angular errors of the X axis are plotted in Fig. 23 and Fig. 24.

The angular error $\varepsilon_x(x)$, was decreased by up to 57% and the $\varepsilon_y(x)$, was decreased by up to 82.5 %. Fig. 25 shows the resulting vertical straightness error $\delta_z(x)$ for the linear axis with compensated angular errors $\varepsilon_x(x)$, $\varepsilon_y(x)$. The vertical straightness was not negatively affected by compensation of angular errors.

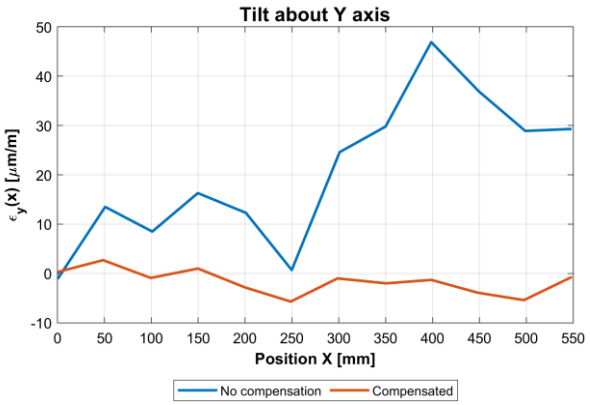

Figure 24. Comparison of tilt error for uncompensated and compensated axis

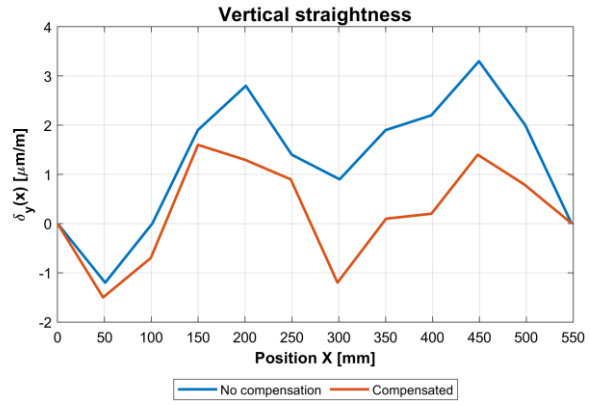

Figure 25. Vertical straightness measured for compensated tilt

5.2 Pseudo compensations

The vertical straightness error of the tested linear axis $\delta_z(x) \leq 5$ µm is better than would be appropriate for initial tests (a larger error would be preferable). In order to test the vertical straightness compensation the assumption that the guiding surface should have an artificial shape was made.

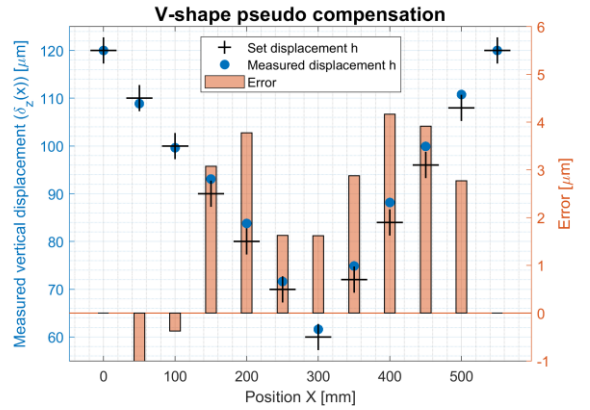

Figure 26. V-shape pseudo compensation

Primitive "V" and "U" shapes were selected. Movement of the worktable around these primitive shapes on a flat guiding surface is further called pseudo compensation. The procedure was similar to angular error compensation. A look-up table with vertical displacement according to the required pseudo compensation was constructed. The previously measured straightness error $\delta_z(x)$ (Fig. 16) was not superimposed to the programmed vertical position of "V" and "U" shapes in the look-up table. The results of the pseudo compensation of the "V" and "U" shapes are plotted in charts in Fig. 26 and Fig. 27, where black crosses denote the set value and blue dots mark the measured value of $\delta_z(x)$ by a Renishaw XM-60 device.

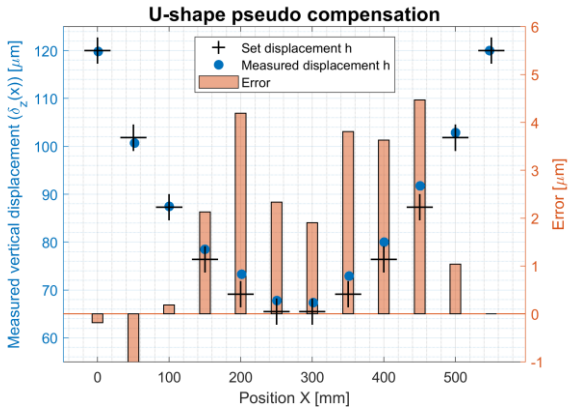

Figure 27. U-shape pseudo compensation

The measurement was quasi-static. The difference between the set and measured values follows the character of the previously measured straightness error $\delta_z(x)$ shown in Fig. 16. The maximal difference between the set and measured values is less than $5\ \mu m$. A smaller error could be achieved if the pseudo compensation table also included straightness error compensation. Here, only the pseudo-compensation table was used for clarity.

6. DISCUSSION

The objective of developing actively controlled HS guideways was to achieve a micro meter and micro radian range of controlled movements of e.g. a worktable of a mid-sized vertical milling centre without adding any compliant (flexible) parts into a machine-tool-workpiece chain. These microscopic movements are intended to serve to correct geometric errors and thermal deformations which manifest as angular errors that cannot be compensated on three-axis machine tools and therefore impair the working accuracy of the machine.

Straightness measurement

The table and bed assembly is statically indeterminate. Each HS block contains preloaded HS pockets (main and preloading pockets). Further, there is force interaction between four HS blocks. Guiding surfaces (prisms) are manufactured with final precision (flatness of $6\ \mu m$). Capillary regulators are also manufactured with errors and thus flow through capillary can vary. In this case, the tolerance for the flow rate was $\pm\ 10\%$. Moreover, the mechanical structure can thermally deform. This leads to elastic deformation of the mechanical structure. Therefore, the gap heights of the HS pockets for capillary regulation change with the X coordinate in Fig. 17. Furthermore, pressure in the main HS pockets that are plotted in Fig. 18 also changes with the X coordinate. The pressure varies significantly from pocket to pocket. The pressure curves have the same pattern. The pattern is clearly visible in the range from $300\ to\ 450\ mm$. For the higher gap height, the higher pressure must be in the main HS pocket. Higher pressure is needed to push back the preloading pocket.

Tilt error

The tilt error is partially caused by the accuracy of position sensors that measure the oil layer thickness. The higher the distance between the gap height sensors, the lower the error of the calculated angle. The distance between the position sensors in the X direction is less than half of the distance between the position sensors in the Y direction (see Fig. 8). Therefore, the error in the measured gap height effects tilt about the Y axis more than tilt about the X axis. The tilt error about the Y axis is approximately double the tilt error about the X axis.

Tilt error over axis stroke

The tilt error about the Y axis is higher than the tilt error about the X axis (both before and after compensation). Before compensation, the difference is $48\ um/m$ and $17\ um/m$ for Y and X respectively. The tilt error may be caused by the geometric inaccuracy of the basic guiding surfaces and error in parallelism of keepers. In further research, we should explore the influence of mechanical errors and production accuracy on the resulting parameters and tilt error of the X and Y axes. From the pressure measured on each main HS pocket (see Fig. 18), it is evident that pressure in the HS pockets differs significantly and has a specific character in the range from $250\ mm$ to $550\ mm$.

Angular error compensation

The angular errors were not fully compensated even though the test was carried out in laboratory conditions. This is because the effect of mechanical compliance of the table, bed, and guide system must be considered. This mechanical system is essentially statically indeterminate and still pre-stressed. Facing HS pockets are pre-stressed (see pairs of facing HS pockets in Fig. 4). Further, there is force interaction between the four HS blocks in the corners of the worktable. Therefore, compensation introduces new inner forces which deform the entire system of linear axis. Two possible approaches are suggested to further improve compensation. First, repeat error measurement and create a new compensation table. This should iteratively lead to a reduction of error. Second, create a computational model of the deformable system and then determine a new compensation table. The computational model of the deformable structure should include the measured dimensional and geometrical errors of the bed and table as well as the nonlinear characteristics of the HS guideway.

The vertical straightness error $\delta_z(x)$ was not negatively affected by compensation of angular errors. In this particular case, there was a slight improvement. However, it cannot be stated that the improvement is generally valid. Only angular error about the X and Y axes was compensated. The improved vertical straightness is only a "side-effect".

Pseudo compensations

Since the vertical straightness error of the tested linear axis $\delta_z(x)\ \leq\ 5\ \mu m$ was small, an assumption was made that the guiding surface has an artificial shape. Primitive "V" and "U" shapes were selected. The movement of the worktable around these primitive forms on the flat guiding surface was later referred to as the pseudo compensation. The path was provided in tabular form as a look-up table. The worktable followed the programmed path with a maximal error of less than $5\ \mu m$. The error corresponds to the measured straightness errors of the tested linear axis. The programmed path did not include correction of the straightness error for clarity. Further accuracy improvement should by possible by superposing the straightness error to the table with the programmed path. However, the straightness error is already comparable to state-of-the-art machine tools (up to approx. $10\ \mu m$) [Holub., 2015, 2020; Kenno, 2020; Liang, 2020; Wei, 2019].

Limitations

The presented range of tilts $\pm 150\ \mu m$ is specific for this particular case. The range depends on the linear axis design, particularly on the distance of the HS blocks and clearance of the HS guideway. However, the possibility of controlling the throttling gap height (oil film thickness) from $60\ \mu m$ to $120\ \mu m$ is generally valid and may even be extended. The tilt and vertical displacement range of the worktable are valid when compensations are used separately. If compensations

are used simultaneously, then the range is decreased. Both vertical displacement compensation and tilt error compensation are performed by changing the throttling gap height that is limited. The range may be also reduced by the load. The measurements were quasi static because of the limitations of the measuring devices. In future research, dynamic tests with real machining are planned.

7. CONCLUSION

Machine tool accuracy is limited by many factors, such as geometry and thermal errors. Currently, errors are reduced, for example, by volumetric compensation. However, if the machine tool only has a linear axis, it is impossible to compensate for angular errors because there is no actuator that could tilt the tool or the workpiece. This paper has shown that it is possible to compensate geometrical linear axis errors by means of an actively controlled hydrostatic (HS) guideway that could be used in machine tools to improve precision. Compensation of vertical straightness $\delta_z(x)$ and tilt errors $\varepsilon_x(x), \varepsilon_y(x)$ was presented. Technically, the oil film thickness was controlled by proportional pressure relief valves even though the valves were not originally intended to control flow. Thanks to this simple and inexpensive solution, it is possible to extend the function of HS pockets with the function of miniature actuators for compensation of angular errors in particular.

The tilt error was not fully compensated even though the test was carried out in laboratory conditions. This is because the effect of mechanical compliance of the table, bed, and guide system must be considered. This system is essentially statically indeterminate and still pre-stressed. Therefore, compensation introduces new inner forces, which newly deform the entire system of linear axis. To further improve compensations, two possible approaches are suggested. First, iteratively repeat error measurement and create a compensation table. Second, create a computational model of the deformable system and then determine a new compensation table.

- Tested compensation range without load
  - Vertical positioning from $60\ to\ 120\ \mu m$
  - Tilt about X axis from $-150\ to\ 150\ \mu m/m$
  - Tilt about Y axis from $-150\ to\ 150\ \mu m/m$
- Error compensation
  - Angular error $\varepsilon_x(x)$ was reduced from $17\ \mu m/m$ to $7\ \mu m/m$
  - Angular error $\varepsilon_y(x)$ was reduced from $48\ \mu m/m$ to $9\ \mu m/m$

at the cost of additional sensors, valves, control hardware and increased HS flow rates, which are induced by higher gap height. Higher oil flows naturally lead to higher energy costs for the hydraulic power unit.

The resulting angular and vertical movement range corresponds to the magnitude of geometrical errors of mid- and even large-sized machine tools. This method of active hydrostatic guideway control could be used to compensate machine tool geometrical errors, especially otherwise uncompensable angular errors.

ACKNOWLEDGMENTS

The authors would like to acknowledge funding support from the Czech Ministry of Education, Youth and Sports under the project CZ.02.1.01/0.0/0.0/16_026/0008404 “Machine Tools and Precision Engineering” financed by the OP RDE (ERDF). The project is also co-financed by the European Union.

REFERENCES

[Abel-Keilhack, 2004] Abel-Keilhack, C. Magnetic Fluids as Medium in Hydrostatic Bearings. Original in German: *Magnetische Flüssigkeiten als Medium in hydrostatischen Lagern*. Location: Vulkan-Verlag GmbH, 2004. (German)

[Bryan, 1990] Bryan, J. International Status of Thermal Error Research [online]. *CIRP Annals - Manufacturing Technology*, 1990 *39*(2), 645–656. https://doi.org/10.1016/S0007-8506(07)63001-7

[Guldbakke, 2006] Guldbakke, J. M., & Hesselbach, J. Development of bearings and a damper based on magnetically controllable fluids. [online] *Journal of Physics: Condensed Matter*, 2006 *18*(38), S2959–S2972. https://doi.org/10.1088/0953-8984/18/38/S29

[Hesselbach, 2003] Hesselbach, J., & Abel-Keilhack, C. Active hydrostatic bearing with magnetorheological fluid. *Journal of Applied Physics*, 2003 *93*(10 3), 8441–8443. https://doi.org/10.1063/1.1555850

[Holub, 2015] Holub, M., Blecha, P., Bradac, F., & Kana, R. Volumetric compensation of three-axis vertical machining centre. *MM Science Journal*, *2015* (OCTOBER), 677–681. https://doi.org/10.17973/MMSJ.2015_10_201534

[Holub, 2020] Holub, M., Jankovych, R., Vetiska, J., Sramek, J., Blecha, P., Smolik, J., & Heinrich, P. (2020). Experimental study of the volumetric error effect on the resulting working accuracy-Roundness. *Applied Sciences (Switzerland)*, *10*(18). https://doi.org/10.3390/APP10186233

[HUANG, 2013] HUANG, H.-C., & Po-Chun, Y. (2013). *Self-compensating hydrostatic journal bearing*. TW. Papent

[Hyprostatik, 2021] Hyprostatik. *PM controller and jet pump*. [online] [2022 11.4.] https://hyprostatik.de/en/products-service/pm-flow-controller-for-guides/

[Hyprostatik, 2022] Hyprostatik. *Advantages over rolling-element bearings*. [online] [2022 11.4.] https://hyprostatik.de/en/technology/advantages-over-rolling-element-bearings/

[Kenno, 2020] Kenno, T., Sato, R., Shirase, K., Natsume, S., Spaan, H. A. M. Influence of linear-axis error motions on simultaneous three-axis controlled motion accuracy defined in ISO 10791-6. *Precision Engineering*, *61*(September 2019), 110–119. https://doi.org/10.1016/j.precisioneng.2019.10.011

[Lazak, 2016] Lazak, T., Stach, E., & Novotny, L. Compensation of Machine Tools Geometrical Errors by means of Actively Controlled Hydrostatic Guideways. In P. Smutny (Ed.), *The 23rd International Conference on Hydraulics and Pneumatics* (pp. 33–39). VSB - Technical University of Ostrava. http://ichp.vsb.cz/

[Lee, 1998] Lee, E. S., Suh, S. H., & Shon, J. W. (1998). A comprehensive method for calibration of volumetric positioning accuracy of CNC-machines. *International Journal of Advanced Manufacturing Technology*, *14*(1), 43–49. https://doi.org/10.1007/BF01179416

[Li, 2020] Li, H., Zhang, P., Deng, M., Xiang, S., Du, Z., & Yang, J. (2020). Volumetric error measurement and compensation of three-axis machine tools based on laser bidirectional sequential step diagonal measuring method. *Measurement Science and Technology*, *31*(5), 055201. https://doi.org/10.1088/1361-6501/AB56B1

[Liang, 2020] Liang, L., Zhang, N., & Peng, C. Development of real-time prediction module for precision and error of CNC system finishing. *Journal of Physics: Conference Series*, *1601*(6). https://doi.org/10.1088/1742-6596/1601/6/062009

[Nakao, 2015] Nakao, Y., Komori, M., Makino, N., Hayashi, A., & Suzuki, K. Displacement control of water hydrostatic thrust bearing by hybrid use of constant resistance restrictors and flow control valve. *Proceedings of the 15th International Conference of the European Society for Precision Engineering and Nanotechnology, EUSPEN 2015*, *June*, 263–264.

[Park, 1998] Park, C. H., & Lee, H. S. *Variable capillary apparatus for hydrostatic bearing and motion error compensating method using same.* (Patent No. US6120004 (A) — 2000-09-19). The United States Patent and Trademark office. [2022 11. 04.] https://worldwide.espacenet.com/publicationDetails/biblio?CC=US&NR=6120004A&KC=A&FT=D&ND=&date=20000919&DB=&locale=#

[Park, 2006] Park, C. H., Oh, Y. J., Shamoto, E., & Lee, D. W. (2006). Compensation for five DOF motion errors of hydrostatic feed table by utilizing actively controlled capillaries. *Precision Engineering*, *30*(3), 299–305. https://doi.org/10.1016/j.precisioneng.2005.10.002

[Patzwald, 2001] Patzwald, R. Magnetic fluids as a lubricant in hydrodynamic plain bearings. Original in German: *Magnetische Flüssigkeitenals Schmierstoff in hydrodynamischen Gleitlagern* Technical University of Berlin. [2022 11. 04.] https://depositonce.tu-berlin.de/items/a7d75d02-96ee-4813-8f05-f6676aa30757

[Ramesh, 2000] Ramesh, R., Mannan, M. A., & Poo, A. N. Error compensation in machine tools - a review. Part I: Geometric, cutting-force induced and fixture-dependent errors. *International Journal of Machine Tools and Manufacture*, *40*(9), 1235–1256. https://doi.org/10.1016/S0890-6955(00)00009-2

[Renn, 2019] Renn, J. C., & Wu, G. Y. A Study on Active Closed-Loop Gap Control for Hydrostatic Bearing. *Applied Mechanics and Materials*, *894*, 51–59. https://doi.org/10.4028/www.scientific.net/amm.894.51

[Schwenke, 2008] Schwenke, H., Knapp, W., Haitjema, H., Weckenmann, A., Schmitt, R., & Delbressine, F. Geometric error measurement and compensation of machines—An update. *CIRP Annals*, *57*(2), 660–675. https://doi.org/10.1016/J.CIRP.2008.09.008

[Slocum, 1992a] Slocum, A. H. *Precision machine design*. Prentice Hall.

[Slocum, 1992b] Slocum, A. H. (1992b). *Self-compensating hydrostatic linear motion bearing*. Patent. [2022 11.04.] https://www.google.com/patents/US5104237

[Stach, 2013] Stach, E., Mares, M., & Sulitka, M. (2013). Comparison of hydrostatic regulation system of thrust bearing of turntable. In P. Smutný (Ed.), *International Conference on Hydraulics and Pneumatics* (p. 9). VSB - Technical University of Ostrava. ISBN 978-80-248-3136-7

[Weck, 1997] Weck, M. Machine tool 2, Original in German: *Werkzeugmaschinen 2*. Springer Berlin Heidelberg. https://doi.org/10.1007/978-3-662-10920-5

[Wei, 2019] Wei, X., Su, Z., Yang, X., Lv, Z., Yang, Z., Zhang, H., Li, X., & Fang, F. A novel method for the measurement of geometric errors in the linear motion of CNC machine tools. *Applied Sciences (Switzerland)*, *9*(16). https://doi.org/10.3390/app9163357

[Yang, 2014] Yang, S., Xu, Y., Sun, L., Yang, L., Liu, S., & Long, X. The Hydrostatic Worktable Performance of an Ultra-precision Optical Aspheric Machine Tool. *Procedia CIRP*, *00*, 187–191. https://doi.org/10.1016/j.procir.2015.04.064

[Zeleny, 1969] Zeleny, J. *Servostatic guideways, a new kind of hydraulically operating guideways for machine tools*. 193–201. https://doi.org/10.1016/b978-0-08-015661-3.50017-5

[Zeleny, 1973] Zeleny, J. (1973). *Control system for machine tool members*. Patent

[Zhang, 2011] Zhang, H., Yang, J., Zhang, Y., Shen, J., & Wang, C. (2011). Measurement and compensation for volumetric positioning errors of CNC machine tools considering thermal effect. *International Journal of Advanced Manufacturing Technology*, *55*(1–4), 275–283. https://doi.org/10.1007/s00170-010-3024-5

[Zollern, 2022] Zollern. *Hydrostatic bearing systems - Plain bearing technology* (p. 20). [online] [2022 11.04.] http://www.zollern.co.kr/Hydrostatic-Bearing-Systems.pdf

CONTACTS:

Tomas Lazak
Czech Technical University in Prague, Faculty of Mechanical Engineering, Department of Production Machines and Equipment (RCMT)
Horska 3, Prague 2, 128 00, Czech Republic
+420 731 628 550, t.lazak@rcmt.cvut.cz,
https://rcmt.cvut.cz/

Eduard Stach, Ph.D.
Czech Technical University in Prague, Faculty of Mechanical Engineering, Department of Production Machines and Equipment (RCMT)
Horska 3, Prague 2, 128 00, Czech Republic
+420 221 990 969, e.stach@rcmt.cvut.cz,
https://rcmt.cvut.cz/

Jan Smolik, Ph.D.
Czech Technical University in Prague, Faculty of Mechanical Engineering, Department of Production Machines and Equipment (RCMT)
Horska 3, Prague 2, 128 00, Czech Republic
+420 221 990 918, j.smolik@rcmt.cvut.cz,
https://rcmt.cvut.cz/

Ivan Divis, Ph.D.
Czech Technical University in Prague, Faculty of Mechanical Engineering, Department of Production Machines and Equipment (RCMT)
Horska 3, Prague 2, 128 00, Czech Republic
+420 221 990 941, i.divis@rcmt.cvut.cz,
https://rcmt.cvut.cz/

Tomas Fornusek, Ph.D.
Czech Technical University in Prague, Faculty of Mechanical Engineering, Department of Production Machines and Equipment (RCMT)
Horska 3, Prague 2, 128 00, Czech Republic
+420 221 990 906, t.fornusek@rcmt.cvut.cz,
https://rcmt.cvut.cz/